Perfluoroalkyl substances in the Yangtze River: Changing exposure and its implications after operation of the Three Gorges Dam

Perfluoroalkyl Substances in the Yangtze River: Changing Exposure and Its Implications after Operation of the Three Gorges Dam

Jie Li[a], Yue Gao[b], Nan Xu[b, *], Bin Li[b], Rui An[a], Weiling Sun[a], Alistair G.L. Borthwick[c], Jinren Ni[a, d**]

[a]*College of Environmental Sciences and Engineering, Peking University, The Key Laboratory of Water and Sediment Sciences, Ministry of Education, Beijing 100871, China*

[b]*Key Laboratory for Heavy Metal Pollution Control and Reutilization, School of Environment and Energy, Peking University Shenzhen Graduate School, Shenzhen 518055, China*

[c]*School of Engineering, The University of Edinburgh, Edinburgh EH9 3JL, United Kingdom*

[d]*School of Environmental Science and Engineering, Southern University of Science and Technology, Shenzhen, China*

*Correspondence to Nan Xu: Tel./Fax: (86) 0755-26035347; E-mail: xunan@pkusz.edu.cn

**Correspondence to Jinren Ni: Tel./Fax: (86) 010-62751185; E-mail: nijinren@iee.pku.edu.cn

ABSTRACT

Potential ecological risk from perfluoroalkyl substances (PFASs) under changing exposure in large river systems is an emerging challenge. Based on systematic monitoring of PFASs at 43 hydrologic stations along a 4300 km continuum of the Yangtze River, we investigated the ecological risk of PFASs under changing exposure resulting from operation of the Three Gorges Dam (TGD). Importantly, perfluorooctanoic acid (PFOA) extensively occurred in most mainstream water samples, accounting for about 90% of the total content of PFASs in both spring and autumn, while short-chain PFASs contributed more than PFOA in sediment. The significant inversion of long-chain PFASs occurrence from sediment to water reflected a profound change in exposure due to loss of finer sediments resulting from long-distance, long-term scour of the riverbed downstream of the TGD. Coarsening of bed materials weakened sorption of long-chain PFASs in sediments and enhanced their exposure in water, resulting in substantial increase of ecological risk to representative aquatic organisms. In the long term, particular attention must be paid to reducing PFOA discharges downstream of the TGD from local industries. The paper also highlights the influence of huge dams on altering river exposure to persistent organic pollutants and the necessity for a new strategy for ecological risk management of large river systems.

***Key words*:** Perfluoroalkyl substances, changing exposure, ecological risk, Three Gorges Dam, Yangtze River

1. Introduction

Perfluoroalkyl substances (PFASs) are a group of artificial chemicals with unique physicochemical properties including surface activity, thermal and acid resistance, and repellency to water and oil. PFASs have been used worldwide for more than 60 years in many applications including stain repellents, food packaging, firefighting foams, textile treatment, metal plating, and semiconductors (Blaine et al., 2013; Wang et al., 2010; Xie et al., 2013). Because of their high-energy carbon-fluorine bonds, PFASs are resistant to hydrolysis, photolysis, and microbial degradation (Kissa, 2001).

PFASs can accumulate in aquatic systems, leading to bioaccumulation and biomagnification through the food chain to wildlife and humans (Loi et al., 2011; Squadrone et al., 2014), and have been detected in rivers, lakes, and oceans (Lee et al., 2020; Li et al., 2020a; Liu et al., 2019) and in wildlife (Pasanisi et al., 2016; Sedlak et al., 2017; Zheng et al., 2020). Notably, PFASs have been found in polar areas (Stroski et al., 2019), demonstrating the long-distance transport of such compounds (Maclnnis et al., 2019). Given their inherent toxicity, PFASs have attracted much attention from scientists and regulators. In order to restrict their global production and use, Annex B of the Stockholm Convention in May 2009 (UNEP, 2009) listed perfluorooctane sulfonic acid (PFOS), its salts, and perfluorooctane sulfonyl fluoride (PFOSF) as persistent organic pollutants. Moreover, perfluorooctanoic acid (PFOA), its salts and PFOA-related compounds have been listed in Annex A of the Stockholm Convention during Conference of Parties in 2019 (Stockholm Convention, 2019). As an unintended consequence, the manufacture of PFASs shifted toward less-regulated, developing countries to meet world demand for unregulated short-chain (usually less than seven fluorinated carbons) and new polyfluorinated homologues (Heydebreck et al., 2015; Su et al.,

2017). Previous studies have reported that perfluorobutane sulfonate (PFBS) was the most abundant substitute chemical found in the surface waters of Tangxun Lake, China, with an average concentration of 3660 ng/L (Zhou et al., 2013), and in the lower Rhine River watershed, Netherlands, the concentration reaching 37 ng/L (Eschauzier et al., 2010). In both cases, a manufacturing plant was responsible for the PFBS pollution.

Many studies aimed at understanding the source, distribution, and composition of PFASs in aquatic environments, such as the Pearl, Haihe, Yangtze, and Hanjiang rivers, and Tangxun, Taihu, and Chaohu lakes in China (Guo et al., 2015; Li et al., 2011; Liu et al., 2016; Pan et al., 2014; So et al., 2007; Wilhelm et al., 2010; Zhou et al., 2013). Li et al. (2020b) concluded that PFASs concentrations in soils are higher in industrialized, urbanized areas than in less-populated, remote regions in China. Although restrictions have been imposed on the manufacturing and use of PFASs, their sustained release to the environment raises serious concerns regarding the toxicity of PFASs to non-target aquatic organisms. In general, effects of PFASs on model-organisms (algae, daphnids, and fish) have been evaluated in order to understand their ecological risks.

The Yangtze River, as the longest river in China, flows more than 6300 km from the Qinghai-Tibet Plateau eastward to the East China Sea. Recently, significant reduction of fine sediment in the riverbed has been observed (Cheng et al., 2013; Yang et al., 2006; Yang et al., 2007) downstream of dams, most notably the Three Gorges Dam (TGD), along the mainstream of the Yangtze River. Yang et al. (2007) quantified the influence of the TGD on downstream sediment delivery and found that although 151 Mt/yr (1 Mt = 10^6 tons) of sediment was retained by TGD after it first began operation (2003-2005), significant erosion of the riverbed occurred further downstream. Yang et al. (2006) forecast that after completion of the TGD in 2009, the sediment load at Datong would

80 decrease to about 210 Mt/yr during the next 20 years. Recent observations show that the total
81 amount of sediment is decreasing in the lower reaches downstream of the dam (Cheng et al., 2013).
82 In general, construction of dam cascades for the regulation of river runoff alters the natural
83 hydrological cycle and downstream sediment transport process (Benn and Erskine, 1994). In the
84 middle and lower reaches of the Yangtze River, the sediment is coarsening because of erosion (Luo
85 et al., 2012; Yang et al., 2014). Sediment coarsening and riverbed erosion were also similarly
86 observed after commissioning of the Iron Gates Dam, River Danube, on the boundary between
87 Serbia and Romania (Panin, 2003) and dams along the Ebro River, Spain (Batalla, 2003). River
88 sediment is an important sink for all kinds of pollutants. However, under certain conditions,
89 pollutants carried by sediment are released back into the surrounding water so that the sediment
90 then becomes a source of water-borne pollutants. This may seriously influence river water quality,
91 leading to secondary water pollution. Through such exchanges of pollutants between sediment and
92 water, aquatic organisms may become exposed to increased risk from higher concentrations of
93 pollutants.
94 Previous studies have focused primarily on PFASs pollution risk in undisturbed aquatic systems,
95 neglecting changes to exposure resulting from human activities. To illustrate the risk resulting from
96 changing exposure, we consider three major scenarios. Risk emanating from PFASs can be
97 understood as an interaction of impacts, exposure, and vulnerability, forming a 'risk triangle'
98 (Crichton, 1999; Lindley et al., 2006) with risk represented by the area of the triangle. The
99 objectives of the present study are: (1) to investigate the contamination profiles, spatial distribution,
100 and partition behavior of 11 PFASs in water and sediment from the Yangtze River; (2) to assess the
101 aquatic environmental risks posed by each compound and the mixture under different scenarios for

changing exposure due to sediment coarsening over ~1000 km downstream; and (3) to give suggestions about the future management of PFASs along the Yangtze River. Organisms in three trophic levels (algae, daphnids, and fish) are selected as references to evaluate the ecological risk. The present study provides an improved understanding of contamination of the Yangtze River by PFASs, and evaluates the increased risk caused by altered exposure arising from anthropogenic impacts, and assists agencies responsible for all stages in the PFASs supply chain.

2. Materials and methods

2.1. Chemicals

Eleven kinds of PFASs were analyzed. Perfluorohexanoic acid (PFHxA), perfluorononanoic acid (PFNA), perfluorodecanoic acid (PFDA), perfluoroundecanoic acid (PFUnDA), perfluorobutane sulfonic acid (PFBS), and perfluorohexane sulfonic acid (PFHxS) of high purity (> 99%) were purchased from J&K (China); perfluoroheptanoic acid (PFHpA, 98%) and perfluorotetradecanoic acid (PFTeDA, 96%) were obtained from Fluorochem (UK); PFOA and PFOS were supplied by AccuStandard (USA) with purity higher than 98%; perfluorododecanoic acid (PFDoA, 98%) were purchased from Matrix (USA); [$^{13}C_8$]-PFOS (98%) and [$^{13}C_8$]-PFOA (98%) were obtained from Cambridge Isotope Laboratories (USA); [$^{13}C_6$]-PFHxA (98%) and [$^{13}C_9$]-PFNA (98%) were purchased from Wellington Laboratories (Canada).

HPLC grade methanol and acetonitrile (ACN) were purchased from Sigma-Aldrich (St. Louis, MO, USA) and J&K (China), respectively. Milli-Q water was obtained from a Millipore system (Millipore, Bedford, MA, USA).

2.2. Sampling

Water and sediment were collected simultaneously at 43 hydrologic stations of the Yangtze River in the spring (March, the dry season) and autumn (October, the flooding season) of 2014. Of the 43 hydrologic stations, 24 sites were located along the 4300 km long mainstream and 19 sites were located in certain key tributaries, including the Jialingjiang, Minjiang, Wujiang, Huangbaihe, and Hanjiang rivers, and Dongting and Poyang lakes (Fig. 1). Table S1 lists details of the sampling locations.

Water samples were collected in 5 L amber polyethylene terephthalate (PET) bottles which were rinsed first with methanol and then with river water at each location before sampling. The water samples were placed in ice bags and transported to nearby laboratories at Chongqing, Yichang, Xiangyang, Wuhan, and Nanjing (depending on the location of the sampling point) for pretreatment within 24 h. Sediment samples were collected either using an iron spade in shallow water or by means of a Peterson grab in deep water, and stored in 1 L aluminium boxes. Upon arrival at the laboratory, the samples were immediately stored in a freezer at -20 ℃. After collection, the pretreatment of water and sediment was as described in Text S1 (supplementary information). For water sample recovery studies, each 2 L Milli-Q water sample was spiked with 1 ml of standard stock solutions at two concentrations (25 and 50 ng/L) respectively. For sediment recovery studies, each 2 g sediment was spiked with 1 ml standards at two concentrations of 25 μg/kg and 50 μg/kg, respectively. Table S2 lists the absolute recoveries obtained for spiked the water and sediment samples.

2.3. Instrument analysis

Target analytes were analyzed using ultrahigh-performance liquid chromatography (UHPLC, 1290, Agilent, USA) interfaced with triple quadrupole mass spectrometry (MS/MS, 6460A, Agilent, USA) operated in electrospray negative ionization mode. The injection volume was 5 μL. PFASs were separated using an Agilent Zorbax Eclipse Plus-C18 (Rapid Resolution HD 2.1×100 mm, 1.8 μm) with a corresponding guard pre-column. The column temperature was set at 40 ℃. The MS/MS parameters were optimized for individual analytes, as shown in Table S3.

The mobile phases for the negative mode were Milli-Q water (A) and ACN (B) at a flow rate of 0.25 mL/min. The mobile phase was initially 90% A and then ramped down from 90% to 10% A in 5 min, maintained constant for 1 min, ramped up to 90% A in 0.1 min, and maintained constant for 5 min. The MS operating conditions were set as follows: gas temperature, 350 ℃; gas flow, 9 mL/min; nebulizer pressure, 35 psi; capillary voltage, 3500 V; and delta EMV, 400 V.

2.4. Setting of scenarios and parameters

Lu et al. (2006) reported that riverbed scour downstream the dam would last for about 50 years after TGD construction. Assuming that the total amount and composition of PFASs released into the Yangtze River from various sources remained constant over this period, the corresponding ecological risk could be evaluated based on three representative scenarios. Scenario No.1 is designed for the past stage before the operation of TGD in 2003; Scenario No.2 denotes the present stage after 10 years' operation of TGD, based on large-scale monitoring conducted in the spring and autumn of 2014; Scenario No.3 represents the future stage after 20 or 50 years' operation of TGD. Other scenarios are also considered, including cases with different PFASs control measures (for different ecological risk reduction targets of 10%, 20%, and 50%, respectively) at different target

years (20, 30, 40 and 50 years) after TGD operation. These scenarios are consistent with governmental efforts in China for reducing PFASs under the framework of the POPs Convention. Meanwhile, particular attention is being paid to reducing contamination level of specific PFASs (e.g. PFOA) according to the local severity of problems encountered in the Yangtze River.

2.5. Ecological risk assessment

Ecological risk assessment (Text S2) was conducted for the different scenarios mentioned above. A model was developed to calculate the partition coefficient (K_d, the concentration of PFASs in the sediment divided by the concentration in the water) and the PFASs concentrations in water under different scenarios (except measurement in 2014) (Text S3).

2.6. Quality control and quality assurance

Data quantification was undertaken by an internal standard calculation method using a series of eight-point calibration curves ($r^2 > 0.99$) (1, 2, 5, 10, 20, 50, 100, 200 μg/L). The limit of detection (LOD) was determined as the concentration that yields a signal/noise (S/N) ratio equal to 3, and the limit of quantification (LOQ) as the concentration that yields a S/N ratio equal to 10 (Table S2). Data below LOD were displayed as zero, while LOD< values <LOQ were assigned with ½ LOQ. Procedural and field blanks all had concentration values below LOD, and the mean recoveries of spiked samples ranged from 70.2% to 122% for water samples and from 31.5% to 106% for sediment (Table S2). Although absolute recoveries were low for three long-chain PFASs, the actual concentrations of these PFASs in the samples were quantified using the internal standard calculation method. Therefore, the internal-standard ([$^{13}C_9$]-PFNA) corrected recoveries of these long-chain

PFASs were about 50%, meeting the requirement of quantitative analysis. Mean recoveries of the four internal standards ([$^{13}C_6$]-PFHxA, [$^{13}C_8$]-PFOA, [$^{13}C_9$]-PFNA and [$^{13}C_8$]-PFOS) were 126%±11.3%, 82.9%±10.1%, 106%±24.9% and 99.9%±18.8 for water samples and 63.8%±14.3%, 94.5%±9.2%, 62.0%±5.3% and 73.0%±6.8% for sediment samples, respectively. Instrument relative standard deviations (RSDs) of intra-day, inter-day and inter-week assays were all below 15%. Concentrations of PFASs in the samples were not corrected for their corresponding recoveries.

2.7. Data analysis

All data analyses were performed using SPSS 20 and Origin 9.1. Heatmaps were produced with R statistical software. Nonmetric multidimensional scaling (NMDS) and analysis of similarities (ANOSIM) were conducted using R statistical software to identify differences between the two seasons (spring and autumn).

3. Results and discussion

3.1. Occurrence and spatiotemporal distribution of PFASs in water samples

The concentration levels of 11 kinds of PFASs (range, mean, median, and detection frequencies) in water are summarized in Table 1 and shown in Fig. 2 (a and b) and Fig. S1 (A and B). Total concentrations of PFASs ranged from 0.30 to 88.50 ng/L in spring and from ND (not detected) to 68.78 ng/L in autumn. The highest overall concentrations (C_{tot} = ∑PFASs) in both seasons were found at ZT, LZ, and CT (Fig. 2 (a and b)). These sites were located close to Luzhou, and Chongqing, both of which are highly developed cities. In the water samples analyzed, PFOA was

212 the predominant PFAS, with concentrations in the range from ND to 86.90 ng/L in spring and in the
213 range from ND to 62.85 ng/L in autumn, with detection frequencies > 90%. These results were
214 consistent with a previous study on waterborne PFASs in the Yangtze River (So et al., 2007). In the
215 present study, PFBS, PFHxS, PFDoA, and PFTeDA were also detected in more than 50% of the
216 water samples. Fig. 2 illustrates the spatial variations in concentrations of PFASs in water, with
217 higher values occurring in the upper reach of the Yangtze mainstream. This should be attributed to
218 the input of certain important point sources, such as the fluorochemical industrial parks along the
219 upper stream near Luzhou and Chongqing (Chen, 2013). Total mean concentrations of PFASs in the
220 mainstream (23.59 ng/L for spring and 17.13 ng/L for autumn) were higher than those in tributaries
221 (4.96 ng/L for spring and 4.62 ng/L for autumn). For example, Wuhan is located along the
222 mainstream, and is also where the Hanjiang tributary joins the Yangtze. Higher concentrations were
223 detected in Wuhan than at other sites along the Hanjiang River. This is primarily because Wuhan is
224 a major city with extensive production of PFASs (Jin et al., 2006; Mei, 2008; Wang et al., 2013).
225 Fig. 2 also depicts the seasonal variation in PFASs, whose total concentration in water was mostly
226 higher ($p<0.05$) in spring (mean = 16.17 ng/L) than in autumn (mean = 11.89 ng/L) due to
227 differences in river flow discharge. On average, the flow rate during the sampling in October was
228 2.9 times that in March (Table S1), diluting the PFASs. NMDS and ANOSIM analyses also showed
229 significant difference between concentrations of PFASs in spring and autumn water samples (Fig.
230 S2). However, the Pearson correlation coefficient for PFOA concentration in both seasons was
231 significant with values of 0.85 ($p<0.01$) in the mainstream and 0.84 ($p<0.01$) in tributary streams
232 (Fig. S3). This reflected the stability of pollution sources of PFOA discharging into the Yangtze
233 River in both seasons. Fig. S4 displays the composition profiles of individual PFASs, with PFOA

making the greatest contributions: 5.17-99.5% in spring, and 0-97.9% in autumn. PFBS and PFOS accounted for 0.14-65.5% and 0-31.2% of total PFASs in spring, and 0.37-63.9% and 0-77.4% in autumn, respectively. Due to the greater contributions of PFOS in autumn, there were obvious differences between the compositions of PFASs in spring and autumn water samples, especially in the upper stream, including the mainstream sites from SG to YB and the tributary sites along the Minjiang, Jialingjiang, and Wujiang rivers (Fig. S4).

Compared with previous studies (Table S4), total concentrations of PFASs in the Yangtze River were lower than those in surface waters of eastern China (Lu et al., 2015), Pearl river, China (Pan et al., 2014), Marina catchment, Singapore (Nguyen et al., 2011), Hanoi city and its surrounding areas, Vietnam (Kim et al., 2013), and Youngsan and Nakdong watershed of South Korea (Hong et al., 2013), but higher than in the Ganges River, India (Sharma et al., 2016). Turning to individual PFAS, the PFOA concentrations in present study were higher than those reported by So et al. (2007) and Jin et al. (2006) (4.10-35.00 ng/L for So et al. in Yichang and Chongqing and 2.80-5.60 ng/L for Jin et al. in Wuhan areas), but lower than eastern China (0-223.8 ng/L) (Chen et al., 2016a). However, for PFOS, Pan and You (2010) reported that the estuary was a sink for PFOS which could reach high concentration of 703.30 ng/L, higher than in the present study. This difference may be due to the prohibition of PFOS since 2009 (UNEP, 2009).

3.2. Occurrence and spatiotemporal distribution of PFASs in sediment

Concentrations of PFASs in the Yangtze River sediment ranged from 9.70 to 151.60 μg/kg in spring and from 1.20 to 96.90 μg/kg in autumn (summarized in Fig. 3 (a and b), Fig. S1 (C and D) and Table 1). PFHxA, PFHpA and PFTeDA were found in all analyzed samples. PFHxA and PFHpA

were the most abundant PFASs in sediment. Measured concentrations of PFHxA ranged from 2.40 to 89.70 μg/kg in spring and from 0.30 to 65.20 μg/kg in autumn, accounting for 43.3% and 50.4% of total mean concentrations of PFASs in sediment. Measured concentrations of PFHpA ranged from 3.20 to 50.80 μg/kg in spring and from 0.20 to 35.50 μg/kg in autumn, accounting for 39.0% and 36.0% of total mean concentrations of PFASs in sediment. The PFHxA and PFHpA concentrations in the present study were higher than those reported previously for the Orge River, France (Labadie and Chevreuil, 2011), Homebush Bay, Sydney, Australia (Thompson et al., 2011), Bohai Sea, China (Chen et al., 2016b), Pearl River, China (Pan et al., 2014) and six major rivers and lakes, South Korea (Lam et al., 2014) (Table S5). Mean concentrations of PFOS were 1.26 μg/kg in spring and 0.13 μg/kg in autumn, which were higher than those reported for Korean rivers (Lam et al., 2014). PFHxA and PFHpA contributed more than PFOA and PFOS to total PFASs in sediment. Considering that PFOA was the predominant PFAS in most mainstream water samples of both seasons, this reflected the significant inversion of long-chain PFASs occurrence from sediment to water. PFHxA is the degradation product of C6 fluorotelomer which can be used to produce C6 fluorotelomer acrylate polymers (ECHA, 2018; Klaunig et al., 2015). PFHpA can be used as waterproof and oil-proof agent in fabrics, and is also a breakdown product of stain and grease proof coatings on couches, food packaging, and carpets (Wang et al., 2015), reflecting use of PFHpA and/or its precursors along the Yangtze River. Another reason may be that PFHxA and PFHpA, as typical short-chain PFASs, show greater transport potential than long-chain PFASs in soils and sediment (Gao and Fu, 2014; Sepulvado et al., 2011). Therefore, short-chain PFASs can migrate deeper into bed sediment once entering the aquatic environment. PFASs can become exposed once the top bed layer is removed. Scouring of the top layer of riverbed sediment may thus have less

effect on the concentration of short-chain than long-chain PFASs in sediment. Previous studies have also conjectured that hydrophobicity is the main mechanism determining the adsorption of PFASs by sediment (Ahrens et al., 2009; You et al., 2010). Besides the hydrophobic effect, electrostatic adsorption and hydrogen bond forces may also promote the adsorption of short-chain PFASs by sediment (Zhao et al., 2012). For further confirmation, the field-based logK_d values in both seasons were calculated for PFASs, using measured concentrations in water and sediment. Only limited logK_d values were available due to undetectable concentrations either in water or in sediment at many sampling sites, and so the calculated logK_d values varied considerably. However, it can still be seen that the field-based logK_d values of PFHxA were in the range of 4.70-5.17 (average 4.94), higher than the mean values of 2.42 reported by Eriksson et al. (2017) and 2.24 reported by Habibullah-Al-Mamun et al. (2016). Field-based logK_d values of PFHpA ranged from 5.35 to 6.16 (average 5.75), higher than the mean value of 2.25 reported by Habibullah-Al-Mamun et al. (2016). Furthermore, field-based logK_d values for PFHxA and PFHpA were higher than those calculated for long-chain PFASs, such as –0.93-2.24 (average 0.72) for PFOA, 1.29-4.52 (average 2.66) for PFOS and 2.21-4.78 (average 3.22) for PFTeDA, suggesting the different effects of riverbed sediment scouring on the partition of short-chain and long-chain PFASs between water and sediment. NMDS and ANOSIM analyses (Fig. S5) showed that the concentration of PFASs in sediment exhibited significant differences ($p<0.01$) between spring and autumn samples. However, little temporal difference was observed for PFASs composition profiles in sediment (Fig. S6).

3.3. Source analysis

Direct sources of PFASs include their production, transportation, use, and disposal in commercial

and daily life. Degradation of precursor compounds provides indirect sources (Prevedouros et al., 2006). In previous studies, PFHpA/PFOA, PFOA/PFNA, and PFOS/PFOA ratios were used to identify pollution sources (Table S6). Simcik and Dorweiler (2005) reported that high values of PFHpA/PFOA (0.26-16) could be used to trace atmospheric deposition of PFASs in surface waters. In the present study, the detected frequency of occurrence of PFHpA was low, with PFHpA/PFOA $\in$ [0, 2.23], indicating a minor contribution by atmospheric deposition. The pollution usually arose through direct emissions from industrial manufacturing processes when PFOA/PFNA $\in$ [2, 15] (Armitage et al., 2009). In the present study, PFOA/PFNA in water ranged from 1.16 (LDX, spring) to 10689 (CLJ, autumn), with mean values of 187.4 in the spring and 1104 in the autumn, far beyond the above range. It is noteworthy that in the upper reaches of the Yangtze, the ratio of PFOS/PFOA was > 1 at several sites, including the mainstream sites from SG to YB, and the tributary sites along the Minjiang, Jialingjiang and Wujiang rivers. This indicated the presence of point sources of PFOS (So et al., 2004). Therefore, such point source inputs of PFOS in the autumn could explain the seasonal composition differences of PFASs in water.

Dozens of commercial activities are located along the Yangtze River, including the Changshu Fluorochemical Industrial Park (Chen et al., 2016a) and fluorochemical industrial parks along the upper stream near Luzhou and Chongqing (Chen, 2013). According to "The 12^{th} five-year development plan of China's fluoride chemical industry" (CAFSI, 2011), fluoropolymer production capacity in China was more than 80,000 tons, accounting for about one third of the world's total production capacity; likewise, fluoropolymer output was nearly 60,000 tons, making China the world's second largest fluoropolymer producer. PFOA is commonly employed as processing acid in the production and application of fluoropolymers used in the chemical, automobile, textile,

322 pharmaceutical, building, electronics, and aviation industries (CAFSI, 2016). Due to the low
323 treatment efficiency of PFASs, contaminated industrial wastewater has entered the Yangtze River
324 and its drainage system. Wang et al. (2010) reported that a single manufacturing facility in Wuhan
325 was the primary source of contamination by PFASs in the region. Liu et al. (2016) also reported that
326 a proposed mega-capacity fluorochemical industrial park could create a risk zone of 10 km radius in
327 terms of surface water pollution by PFASs. Liu et al. (2017) estimated that 70-80% of PFOS/PFOA
328 in central and eastern China came directly from manufacturing and industrial sites, mostly as
329 wastewater. Industrial effluent discharge is therefore the main pollution source of PFASs entering
330 the Yangtze River. Meanwhile, the Yangtze River tributaries act as input point sources that inject
331 contaminants from indigenous manufacturing industries into the Yangtze River. Wang et al. (2013)
332 reported that the flux of PFASs from Hanjiang River to the Yangtze River was 346.1 kg/yr. This
333 underlines why tributary runoff and its contamination by industrial wastewater must be taken into
334 consideration by decision makers.
335 Municipal wastewater usually contains high levels of PFASs due to the daily use of PFAS-
336 containing products and the ineffective scavenging performance of conventional wastewater
337 treatment processes. In China, serious contamination by PFASs has been observed in the influent
338 and effluent of 28 municipal WWTPs located in large cities such as Wuhan and Nanjing (Zhang et
339 al., 2013) and Shenyang (Sun et al., 2011). Given that several mega-cities are located along the
340 Yangtze River, such as Chongqing, Wuhan, Nanjing, and Shanghai, there is a major risk of pollution
341 by PFASs through discharge of municipal wastewater effluent into the Yangtze River.
342
343 **3.4. Individual and mixture risk quotients under the three scenarios**

Considering the effects of the operation of TGD on riverbed scouring and sediment coarsening, and the consequent partitioning of pollutants, three major scenarios were used to estimate the ecological risks of PFASs resulting from changing exposure along the Yangtze River. Ecological risk was assessed from chronic toxicity data (Table S7) for PFASs determined by EPI Suite (EPIWEB v.4.1, The United States Environmental Protection Agency (USEPA)). Fig. 4 shows the mixture risk quotients (MRQs) relating to PFASs in spring water for different scenarios.

3.4.1 Scenario No.1: prior to TGD operation (2003)

We first considered PFASs in the Yangtze before operation of TGD. In this case, the concentrations were calculated based on established models (Text S3). The results derived from risk quotient analysis at three trophic levels (RQ << 0.01) indicated that there was negligible risk from either individual or mixtures of PFASs (Fig. S7 and Fig. 4). It should be pointed out that this prediction was based on an assumption that the total amount and composition of PFASs released into the Yangtze River from various sources remained constant over 50 years after TGD construction. In fact, the concentrations and risks of PFASs in 2003 should be lower than our predictions. Since 2003, national annual production greatly increased to accommodate both domestic and ongoing overseas demands for PFASs (Xie et al., 2013). For example, commercial production of PFOS commenced in 2003 with a total quantity below 50 tons (MEPC, 2008). Annual production of PFOS-related chemicals grew rapidly from 2003 to 2006, reaching approximately 250 tons at the peak (Zhang et al., 2012).

3.4.2 Scenario No.2: post TGD operation based on monitoring in 2014

At most sampling sites, individual RQ was << 0.01, indicating hardly any ecological risk from PFASs. The concentration of PFOA was about one or two orders of magnitude higher than that of PFOS and the risks to fish from PFOA and PFOS were 7.43×10^{-4}-3.54×10^{-3} and 1.23×10^{-5}-$4.07\times10^{-}$

366 ^{5}. In another study, Lin et al. (2010) reported that the risk quotients for PFOA and PFOS in Taiwan's
367 WWTPs and downstream rivers ranged from 1.30×10^{-5} to 4.13×10^{-4} and 8.28×10^{-3} to 0.24,
368 respectively, the values a little higher than the present study. MRQs relating to 11 types of PFASs
369 were $\in$ [7.43×10^{-4}, 0.009] for fish, $\in$ [6.67×10^{-3}, 0.0054] for daphnids, and $\in$ [1.32×10^{-4}, $7.98\times^{-}$
370 ^{4}] for algae. MRQs were all below 0.01 for these three organisms, indicating that, at actual
371 environmental levels, these mixtures of PFASs pose no ecological risk.
372 MRQs allow simple assessment of the overall risk of given pollutants in a large river. However,
373 dam operation may affect the distribution of risk posed by PFASs. For example, the operation of
374 TGD after 2003 has resulted in sediment deposition immediately before the dam, followed by
375 downstream riverbed erosion and sediment coarsening (Guo and He, 2011; Luo et al., 2012; Miao et
376 al., 2016; Xu and Milliman, 2009; Yang et al., 2014). Miao et al. (2016) showed that the sediment
377 mean grain size deposited after 2003 became significantly larger than that deposited during 1988-
378 2002. Guo and He (2011) also reported that suspended sediment mostly consisted of clay and silt,
379 whereas the bed sediment comprised sand in the middle and lower Yangtze River. At the Yichang
380 station, 40 km downstream of TGD, the bed sediment was much coarser, consisting of gravel and
381 pebbles (medium size 24.6 mm). Further downstream from Yichang to Chenglingji, the bed
382 sediment comprised coarse and finer sands (median diameter $\in$ [83, 433] μm). Coarsening was
383 most acute immediately downstream of the TGD (Xu et al., 2010). Partitioning plays an important
384 role in the fate of PFASs in environmental matrixes; and partitioning of PFASs between water and
385 sediment can be assessed by means of a distribution coefficient (K_d, L/kg). Tables S10 and S11 list
386 the estimated values of sediment median size and logK_d values downstream of the TGD for different
387 scenarios. It can be seen that the downstream logK_d values decreased with time. This implies that

388 the interaction between PFASs and sediment weakened due to scouring and sediment coarsening
389 with the presence of the dam. During the flushing process, PFASs are likely to be washed off
390 sediment and aquatic organisms subject to greater exposure, leading to increased ecological risk.

391 **3.4.3 Scenario No.3: TGD operation after 20 years and 50 years**

392 To estimate the ecological risk potentially encountered post-operation of TGD, we considered two
393 cases, namely 20 years and 50 years after operation of TGD. According to the forecast values of RQs
394 and MRQs (taking 50 years after operation of TGD as an example), it is obvious that PFTeDA is
395 likely to be an increasing threat to aquatic organisms, noting its highest values of 3.31 for fish and
396 0.98 for daphnids in the worst case (Fig. S7). The median effect concentration (EC50) of PFTeDA is
397 1 to 4 orders of magnitude lower than other PFASs (Table S7). Hence, PFTeDA (C=14), a typical
398 long-chain compound is likely to pose low to high risk to aquatic organisms (algae RQs: 2.34×10^{-4}-
399 0.059, daphnids RQs: 0.0039-0.98, fish RQs: 0.01-3.31). PFHxA, PFHpA, PFOS, PFDA, PFUnDA
400 and PFDoA appear low risk to daphnids and fish (Fig. S7). These findings are useful in helping
401 prioritize possible remediation activities concerning PFASs in the Yangtze River downstream of the
402 TGD. Further research is needed regarding long-chain PFASs (such as PFTeDA) which are more
403 toxic and pose greater risk than short-chain ones (Kudo et al., 2001; Ohmori et al., 2003; Shi et al.,
404 2009). Although PFBS (a short-chain substitute for PFOS) seem relatively risk-free at future levels
405 from the perspective of an instantaneous concentration, its presence should not be ignored; this is
406 because short-chain PFASs gradually accumulate in the environment. It is worth noting that short-
407 chain PFASs have higher bioavailability because they can pass through the human placenta from
408 mother to baby more easily than long-chain PFASs (Needham et al., 2010).
409 We next estimated MRQ for mixture of PFASs, accounting for the variety present in the aquatic

environment which can lead to overall toxicity greater than that of an individual constituent. Although individual components might be present at concentrations too low to cause concern, additive or even synergistic effects may occur that would result in higher toxicity than a single compound (Schwarzenbach et al., 2006). For the mixture risk, MRQ was > 0.01 (fish) for all sampling sites, indicating low to high risk. For daphnids, YC, SS and CLJ displayed median or high risks. Low risk was forecast for algae at these three sites, located near TGD.

By considering the mixture risks to algae, daphnids, and fish for the three scenarios in Fig. 4, we find that the risk posed by PFASs immediately downstream of the TGD is likely to increase in the future, especially at YC. Fish were found to be more sensitive to PFASs than algae or daphnids, noting that PFASs tend to accumulate in fat. In the "risk triangle" formed by impact, exposure, and vulnerability (Crichton, 1999; Lindley et al., 2006), impact refers to the compositions and concentrations of PFASs, and vulnerability means the tolerance (EC50) of target organisms (algae, daphnids and fish). It is likely that the flushing modes of the TGD will cause finer bed-sediment increasingly to be washed downstream. The resultant coarsening of bed material would weaken the sorption of long-chain PFASs in sediment and strengthen their aquatic occurrence, resulting in increased exposure of representative aquatic organisms to higher levels of PFASs in water, and thereby enhanced ecological risk as defined by the area of the triangle. In natural rivers, there is increased risk of exposure of aquatic organisms to hydrophobic organic compounds caused by the operation of large dams and the consequent coarsening of downstream bed sediment. For similar exposure changes in large rivers, the most effective countermeasure for risk reduction would be to control the source of long-chain PFASs.

3.5. **Reduction plans for PFASs**

3.5.1 Reduction of the total input of PFASs

Now let us further consider further scenarios after implementation of proposed control measures. For similarity, we chose the most sensitive species (fish) as the target organism by which to evaluate how different control measures would influence the ecological risk of PFASs over a period of 50 years after impoundment of TGD. By assuming abrupt decadal reductions of 20%, 50%, and 80% in concentration of PFASs to Yangtze River, we can see that a reduction of 80% is required to ensure MRQs<1 downstream of the TGD (Fig. 5a), especially at sites close to TGD (such as YC, SS, CLJ, and JJ) that are undergoing enhanced exposure to PFASs because of the erosion of fine sediment. Among individual PFAS, PFTeDA accounted for the largest proportion of total MRQs (Fig. 5b), implying that long chain PFASs must be controlled as a matter of top priority. Besides PFTeDA, risk from PFOA accounts for about 40% of the total between DT and XLJ after 50 year operation of TGD (Fig. 5c). Given that PFOA is a newly identified compound of POPs in the Stockholm Convention, particular attention should be paid to reducing PFOA in the Yangtze River in future years.

3.5.2 Reduction rate of PFASs per decade

The USEPA (2006) required eight major manufacturers of PFASs to eliminate PFOA from emissions and product catalogs no later than 2015. As a party to the Stockholm Convention, Chinese government has made great efforts to control the production of PFASs. In September 2019, the Ministry of Ecology and Environment of the People's Republic of China issued a document about production, use, and replacement of PFASs (MEEPRC, 2019) which predicted that pollution levels would reduce as yield decreased. To achieve a risk-free goal in the near future, the efficiency

454 of PFASs control measures is important. We therefore consider three scenarios involving abrupt
455 reductions in PFASs of 10%, 20% and 50% per decade since 2015 to examine the effect on MRQs
456 after 20, 30, 40, and 50 years of TGD operation (Fig. 5 and Fig. S8). Figs. 5d and 5e show that, on
457 abrupt 10% and 20% reductions in PFASs per decade, MRQs are nevertheless larger than unity 20
458 and 50 years after operation of TGD. The target whereby MRQs < 1 throughout the whole reach
459 downstream of TGD is only achieved 50 years after the operation of TGD for a reduction rate in
460 PFASs of 50% per decade (Fig. 5f). This implies that the control efficiency of FFCs should be
461 strengthened to compensate for the risk of changing exposure caused by sediment erosion
462 downstream of the TGD.

463 **3.5.3 Suggestions for industrial source control of PFASs along the Yangtze**

464 Industry involved in manufacture and application of fluoropolymers is the largest source of PFOA
465 in China (Meng et al., 2018). To lower environmental levels of PFOA, source control measures
466 should be focused on relevant industries in major cities along the mainstream of the Yangtze River
467 (Table S8). According to cluster analysis based on 8 industry categories, the primary industries
468 along the Yangtze River comprise electric machinery and equipment, and metal product industries
469 (Fig. 6). Major cities were classified into 6 groups according to their industries, with Groups A and
470 F mainly referring to cities located downstream of TGD. Cities in Group A had a large proportion of
471 industries related to metal products, electric machinery and equipment, and chemical and
472 pharmaceutical products. Shanghai (XLJ in Group F), located on the Yangtze Delta, hosted industry
473 valued at 2276.4 billion yuan (Table S8), mainly comprising electric machinery and equipment, and
474 automobile enterprises. Groups B, D, and E include cities located along the upper and middle
475 reaches of the mainstream in Sichuan, Yunnan, and Hubei provinces, where the primary industries

476 involve metal products, chemical and pharmaceutical products, and food processing and production.
477 Cities in Group C host automobile, electrical machinery, and electrical equipment industries, the
478 most notable example being Chongqing (Eeworld, 2018). Hubei Province is presently the sixth
479 largest automobile manufacturing base in China, with its large automobile industry centered in
480 Wuhan (WH) (Fang et al., 2017).
481 To strengthen measures for reducing sources of PFASs along the Yangtze, top priority should be
482 given to controlling the release of highly toxic, long chain PFASs, such as PFTeDA. Great
483 importance should be attached to regulation of PFOA, which experiences enhanced exposure in
484 water caused by erosion of fine sediment downstream of the TGD and has recently been listed in
485 the Stockholm Convention as a new POP compound. Under the assumed scenarios, a reduction of
486 80% in quantity or 50% in emission rate per decade of PFASs is required to achieve a risk-free
487 situation over the whole reach downstream of the TGD in a 50 year-period after the operation of the
488 dam. Metal products should be the key industry for mitigation measures when drawing up reduction
489 plans for PFASs in Yunnan, Hubei, Anhui, and Jiangsu provinces. Policy makers should pay careful
490 attention to cleansing emissions from motor manufacture, electrical machinery, and electrical
491 equipment industries in Sichuan Province, Chongqing, Wuhan and Shanghai. Integrated
492 countermeasures are urgently needed after the changes in exposure to PFASs that have occurred
493 since operation of TGD commenced in 2003. This will require substantial strengthening and
494 enforcement of industry-specific and city-specific regulations, leading to enhanced reduction rates
495 in PFASs along the whole Yangtze River.
496

497 **4. Conclusions**

Based on a systematic analysis of occurrence, spatiotemporal distribution, and sources of PFASs along a 4300 km continuum of the Yangtze River, we assessed the enhanced risk caused by the changing exposure of aquatic organisms to PFASs in the decades following operation of the TGD. Our study revealed that PFOA was the dominant PFAS in all water samples during both spring and autumn, while PFHxA and PFHpA made the largest contributions to the total PFASs concentrations in sediment. Operation of the TGD has resulted in the continuous coarsening of sediment material over ~1000 km downstream. Risk quotients calculated for past stage (before operation of TGD in 2003), present stage (in 2014), and future stage scenarios indicate that the ecological risk induced by PFASs is likely to grow, due to increased exposure resulting from long-distance, long-term scouring downstream of the TGD. This highlights the urgent need for stricter source control of long-chain PFASs such as PFOA from relevant industries (electrical machinery and equipment, metal products, and chemical and pharmaceutical products) under changing exposure in the Yangtze River basin.

Declaration of interests

The authors declare no conflicts of interest.

Acknowledgments

Funding for this study was provided by the National Science Foundation of China (NSFC) (Grant No. 51721006 and 51579003).

Appendix A. Supplementary data

520 Supplementary data related to this article are attached.

521

522 **References**

523 Ahrens, L., Yamashita, N., Yeung, L.W.Y., Taniyasu, S., Horii, Y., Lam, P.K.S., Ebinghaus, R.,
524 2009. Partitioning behavior of per-and polyfluoroalkyl compounds between pore water and
525 sediment in two sediment cores from Tokyo Bay, Japan. Environ. Sci. Technol. 43, 6969-6975.
526 https://doi.org/10.1021/es901213s.

527 Armitage, J.M., MacLeod, M., Cousins, I.T., 2009. Comparative assessment of the global fate and
528 transport pathways of long-chain perfluorocarboxylic acids (PFCAs) and
529 perfluorocarboxylates (PFCs) emitted from direct sources. Environ. Sci. Technol. 43, 5830-
530 5836. https://doi.org/10.1021/es900753y.

531 Batalla, R.J., 2003. Sediment deficit in rivers caused by dams and instream gravel mining. A review
532 with examples from NE Spain. Cuaternario y Geomorfol. 17 (3-4), 79-91.

533 Benn, P.C., Erskine, W.D., 1994. Complex channel response to flow regulation: Cudgegong River
534 below Windamere Dam, Australia. Appl. Geogr. 14, 153-168. https://doi.org/10.1016/0143-
535 6228(94)90058-2.

536 Blaine, A.C., Rich, C.D., Hundal, L.S., Lau, C., Mills, M.A., Harris, K.M., Higgins, C.P., 2013.
537 Uptake of perfluoroalkyl acids into edible crops via land applied biosolids: Field and
538 greenhouse studies. Environ. Sci. Technol. 47, 14062-14069.
539 https://doi.org/10.1021/es403094q.

540 Chen, H., Sun, R., Zhang, C., Han, J., Wang, X., Han, G., He, X., 2016b. Occurrence, spatial and
541 temporal distributions of perfluoroalkyl substances in wastewater, seawater and sediment from
542 Bohai Sea, China. Environ. Pollut. 219, 389-398. http://doi.org/10.1016/j.envpol.2016.05.017.

543 Chen H.C., 2013. Recent situation of production technology in fluorine chemical industry. Organo-
544 fluor. Ind. 3, 55-57. (in Chinese)

545 Chen, S., Jiao, X.C., Gai, N., Li, X.J., Wang, X.C., Lu, G.H., Piao, H.T., Rao, Z., Yang, Y.L., 2016a.
546 Perfluorinated compounds in soil, surface water, and groundwater from rural areas in eastern
547 China. Env. Pollut. 211, 124-131. https://doi.org/10.1016/j.envpol.2015.12.024.

548 Cheng, L., Jue, Y. S., Yun, H., Hirshfield, F., 2013. Changes in runoff and sediment load from major

549 chinese rivers to the Pacific Ocean over the period 1955-2010. J. Sediment Res. 28, 486-495.
550 https://doi.org/10.1016/S1001-6279(14)60007-X.
551 China Association of Fluorine and Silicone Industry (CAFSI), 2011. Twelfth Five Year Plan for
552 Fluorine Chemical Industry Development in China.
553 https://wenku.baidu.com/view/381c8e2cbd64783e09122bc6.html (accessed 11 February 2020)
554 China Association of Fluorine and Silicone Industry (CAFSI), 2016. Thirteenth Five Year Plan for
555 Fluorine Chemical Industry Development in China.
556 https://wenku.baidu.com/view/2fff66d8f111f18582d05a30.html?rec_flag=default&sxts=15785
557 58245125 (accessed 11 February 2020)
558 Crichton, D. 1999. The risk triangle. Natural disaster management 102, 103.
559 Eeworld, 2018. Chongqing's two pillar industries: electronics VS cars, which is the leader.
560 http://news.eeworld.com.cn/qcdz/2018/ic-news081023491.html (accessed 11 February 2020)
561 Eriksson, U., Haglund, P., Kärrman, A., 2017. Contribution of precursor compounds to the release
562 of per- and polyfluoroalkyl substances (PFASs) from waste water treatment plants (WWTPs).
563 J. Environ. Sci. 61, 80-90. https://doi.org/10.1016/j.jes.2017.05.004.
564 Eschauzier, C., Haftka, J., Stuyfzand, P.J., de Voogt, P., 2010. Perfluorinated compounds in
565 infiltrated river Rhine water and infiltrated rainwater in coastal dunes. Environ. Sci. Technol.
566 44, 7450-7455. https://doi.org/10.1021/es100471z.
567 European Chemical Agency (ECHA), 2018. ECHA opened its second SVHC consultation in 2018
568 on six proposals. https://www.sgsgroup.com.cn/en/news/2018/09/safeguards-12818-echa-
569 opened-its-second-svhc-consultation-in-2018-on-six-proposals? (accessed 11 February 2020)
570 Fang, C.Y., 2017. Developing strategy for automobile industry in Hubei Province. Journal of
571 Wuhan Institute of Shipbuilding Technology 4, 56-59. (in Chinese)
572 Gao, Y., Fu, J., 2014. Spatial and vertical distribution of perfluoroalkyl substances in soil cores
573 around manufacturing facilities in China. Environ. Chem. 33, 1686-1691. (in Chinese)
574 Guo, C., Zhang, Y., Zhao, X., Du, P., Liu, S., Lv, J., Xu, F., Meng, W., Xu, J., 2015. Distribution,
575 source characterization and inventory of perfluoroalkyl substances in Taihu Lake, China.
576 Chemosphere 127, 201-207. https://doi.org/10.1016/j.chemosphere.2015.01.053.
577 Guo, L., He, Q., 2011. Freshwater flocculation of suspended sediments in the Yangtze River, China.
578 Ocean Dyn. 61, 371-386. https://doi.org/10.1007/s10236-011-0391-x.

579 Habibullah-Al-Mamun, M., Ahmed, M.K., Raknuzzaman, M., Islam, M.S., Negishi, J., Nakamichi,
580 S., Sekine, M., Tokumura, M., Masunaga. S., 2016. Occurrence and distribution of
581 perfluoroalkyl acids (PFAAs) in surface water and sediment of a tropical coastal area (Bay of
582 Bengal coast, Bangladesh). Sci. Total Environ. 571, 1089-1104.
583 https://doi.org/10.1016/j.scitotenv.2016.07.104.
584 Heydebreck, F., Tang, J.H., Xie, Z,Y., Ebinghaus, R., 2015. Alternative and legacy perfluoroalkyl
585 substances: Differences between European and Chinese river/estuary systems. Environ. Sci.
586 Technol. 49 (14), 8386-8395. https://10.1021/acs.est.5b01648.
587 Hong, S., Khim, J.S., Park, J., Kim, M., Kim, W.K., Jung, J., Hyun, S., Kim, J.G., Lee, H., Choi,
588 H.J., Codling, G., Giesy, J.P., 2013. In situ fate and partitioning of waterborne perfluoroalkyl
589 acids (PFAAs) in the Youngsan and Nakdong River Estuaries of South Korea. Sci. Total
590 Environ. 445, 136-145. http://doi.org/10.1016/j.scitotenv.2012.12.040.
591 Jin, Y., Ding, M., Zhai, C., 2006. An investigation of the PFOS and PFOA pollution in Three Gorges
592 Reservoir areas of the Yangtze River and surface water of Wuhan areas. Ecol. Environ. 15,
593 486-489. (in Chinese).
594 Kim, J.W., Tue, N.M., Isobe, T., Misaki, K., Takahashi, S., Viet, P.H., Tanabe, S., 2013.
595 Contamination by perfluorinated compounds in water near waste recycling and disposal sites
596 in Vietnam. Environ. Monit. Assess. 185, 2909-2919. https://doi.org/10.1007/s10661-012-
597 2759-x.
598 Kissa, E., 2001. Fluorinated surfactants and repellents. CRC Press.
599 Klaunig, J.E., Shinohara, M., Iwai, H., Chengelis, C.P., Kirkpatrick, J.B., Wang, Z., Bruner, R.H.,
600 2015. Evaluation of the chronic toxicity and carcinogenicity of perfluorohexanoic acid
601 (PFHxA) in Sprague-Dawley Rats. Toxicol. Pathol. 43, 209-220.
602 https://doi.org/10.1177/0192623314530532.
603 Kudo, N., Suzuki, E., Katakura, M., Ohmori, K., Noshiro, R., Kawashima, Y., 2001. Comparison of
604 the elimination between perfluorinated fatty acids with different carbon chain length in rats.
605 Chem. Biol. Interact. 134, 203-216. https://doi.org/10.1016/S0009-2797(01)00155-7.
606 Labadie, P., Chevreuil, M., 2011. Partitioning behaviour of perfluorinated alkyl contaminants
607 between water, sediment and fish in the Orge River (nearby Paris, France). Environ. Pollut.
608 159, 391-397. https://doi.org/10.1016/j.envpol.2010.10.039.

609 Lam, N.H., Cho, C.R., Lee, J.S., Soh, H.Y., Lee, B.C., Lee, J.A., Tatarozako, N., Sasaki, K., Saito,
610 N., Iwabuchi, K., Kannan, K., Cho, H.S., 2014. Perfluorinated alkyl substances in water,
611 sediment, plankton and fish from Korean rivers and lakes: A nationwide survey. Sci. Total
612 Environ. 491, 154-162. http://doi.org/10.1016/j.scitotenv.2014.01.045.
613 Lee, Y.M., Lee, J.Y., Kim, M.K., Yang, H., Lee, J.E., Son, Y., Kho, Y., Choi, K., Zoh, K.D., 2020.
614 Concentration and distribution of per- and polyfluoroalkyl substances (PFAS) in the Asan Lake
615 area of South Korea. J. Hazard. Mater. 381, 120909. http://10.1016/j.jhazmat.2019.120909.
616 Li, F., Sun, H., Hao, Z., He, N., Zhao, L., Zhang, T., Sun, T., 2011. Perfluorinated compounds in
617 Haihe River and Dagu drainage canal in Tianjin, China. Chemosphere 84, 265-271.
618 https://doi.org/10.1016/j.chemosphere.2011.03.060.
619 Li, J.F., He, J.H., Niu, Z.G., Zhang, Y., 2020b. Legacy per- and polyfluoroalkyl substances (PFASs)
620 and alternatives (short-chain analogues, F-53B, GenX and FC-98) in residential soils of China:
621 Present implications of replacing legacy PFASs. Environ. Int. 135, 105419.
622 https://doi.org/10.1016/j.envint.2019.105419.
623 Li, Y., Feng, X., Zhou, J., Zhu, L., 2020a. Occurrence and source apportionment of novel and
624 legacy poly/perfluoroalkyl substances in Hai River basin in China using receptor models and
625 isomeric fingerprints. Water Res. 168, 115145. https://doi.org/10.1016/j.watres.2019.115145.
626 Lin, A.Y.C., Panchangam, S.C., Ciou, P.S., 2010. High levels of perfluorochemicals in Taiwan's
627 wastewater treatment plants and downstream rivers pose great risk to local aquatic ecosystems.
628 Chemosphere 80, 1167-1174. https://doi.org/10.1016/j.chemosphere.2010.06.018.
629 Lindley, S.J., Handley, J.F., Theuray, N., Peet, E., Mcevoy, D., 2006. Adaptation strategies for
630 climate change in the urban environment: assessing climate change related risk in UK urban
631 areas. J. Risk Res. 9 (5), 543-568. https://doi.org/10.1080/13669870600798020.
632 Liu, Y., Zhang, Y., Li, J., Wu, N., Li, W., Niu, Z., 2019. Distribution, partitioning behavior and
633 positive matrix factorization-based source analysis of legacy and emerging polyfluorinated
634 alkyl substances in the dissolved phase, surface sediment and suspended particulate matter
635 around coastal areas of Bohai Bay, China. Environ. Pollut. 246, 34-44.
636 https://doi.org/10.1016/j.envpol.2018.11.113.
637 Liu, Z., Lu, Y., Wang, P., Wang, T., Liu, S., Johnson, A.C., Sweetman, A.J., Baninla, Y., 2017.
638 Pollution pathways and release estimation of perfluorooctane sulfonate (PFOS) and

perfluorooctanoic acid (PFOA) in central and eastern China. Sci. Total Environ. 580, 1247-1256. https://doi.org/10.1016/j.scitotenv.2016.12.085.

Liu, Z., Lu, Y., Wang, T., Wang, P., Li, Q., Johnson, A.C., Sarvajayakesavalu, S., Sweetman, A.J., 2016. Risk assessment and source identification of perfluoroalkyl acids in surface and ground water: spatial distribution around a mega-fluorochemical industrial park, China. Environ. Int. 91, 69-77. https://doi.org/10.1016/j.envint.2016.02.020.

Loi, E.I., Yeung, L.W., Taniyasu, S., Lam, P.K., Kannan, K., Yamashita, N., 2011. Trophic magnification of poly- and perfluorinated compounds in a subtropical food web. Environ. Sci Technol. 45, 5506-5513. https://doi.org/10.1021/es200432n.

Lu, J., Huang, Y., Gong, P., 2006. Changes of scour after the Three Gorge Dam in the middle and lower reaches of the Yangtze River. Yangtze River 09, 55-57. (in Chinese)

Lu, Z., Song, L., Zhao, Z., Ma, Y., Wang, J., Yang, H., Ma, H., Cai, M., Codling, G., Ebinghaus, R., Xie, Z., Giesy, J.P., 2015. Occurrence and trends in concentrations of perfluoroalkyl substances (PFASs) in surface waters of eastern China. Chemosphere 119, 820-827. https://doi.org/10.1016/j.chemosphere.2014.08.045.

Luo, X.X., Yang, S.L., Zhang, J., 2012. The impact of the Three Gorges Dam on the downstream distribution and texture of sediments along the middle and lower Yangtze River (Changjiang) and its estuary, and subsequent sediment dispersal in the East China Sea. Geomorphology 179, 126-140. https://doi.org/10.1016/j.geomorph.2012.05.034.

Maclnnis, J.J., Lehnherr, I., Muir, D.C.G., Piere, K.A.S., Louis, V.L.S., Spencer, C., Silva, A.O.D., 2019. Fate and transport of perfluoroalkyl substances from snowpacks into a lake in the high Arctic of Canada. Environ. Sci. Technol. 53 (18), 10753-10762. https://10.1021/acs.est.9b03372.

Mei, S.F., 2008. Production and usage of PFOS and PFOA in China and current status of domestic and international standards. Organo-fluor. Ind. 1, 21-25. (in Chinese)

Meng, J., Wang, T., Song, S., Wang, P., 2018. Tracing perfluoroalkyl substances (PFASs) in soils along the urbanizing coastal area of Bohai and Yellow Seas, China. Environ. Pollut. 238, 404-412. https://doi.org/10.1016/j.envpol.2018.03.056.

Miao, A., Chu, Z., Li, Y., 2016. Three Gorges Dam controls sediment coarsening of the mud patch on the inner East China Sea shelf. J. Ocean Univ. China 15, 414-422.

669 https://doi.org/10.1007/s11802-016-2798-y.
670 Ministry of Ecology and Environment of the People's Republic of China (MEEPRC), 2019. Notice
671 on public solicitation for information on the production, use and replacement of 6 types of
672 persistent organic pollutants, including short-chain chlorinated paraffins.
673 http://www.mee.gov.cn/xxgk2018/xxgk/xxgk06/201909/t20190924_735346.html. (accessed 20
674 April 2020)
675 Ministry of Environmental Protection of China (MEPC), 2008. Additional information on
676 production and use of PFOS.
677 http://chm.pops.int/Portals/0/Repository/addinfo_2008/UNEPPOPS-POPRC-SUB-F08-PFOS-
678 ADIN-CHI.English.pdf. (accessed 20 April 2020)
679 Needham, L.L., Grandjean, P., Heinzow, B., Jørgensen, P.J., Nielsen, F., Patterson Jr, D.G., Sjödin,
680 A., Turner, W.E., Weihe, P., 2010. Partition of environmental chemicals between maternal and
681 fetal blood and tissues. Environ. Sci. Technol. 45, 1121-1126.
682 https://doi.org/10.1021/es1019614.
683 Nguyen, V.T., Reinhard, M., Karina, G.Y.H., 2011. Occurrence and source characterization of
684 perfluorochemicals in an urban watershed. Chemosphere 82, 1277-1285.
685 http://dx.doi.org/10.1016/j.chemosphere.2010.12.030.
686 Ohmori, K., Kudo, N., Katayama, K., Kawashima, Y., 2003. Comparison of the toxicokinetics
687 between perfluorocarboxylic acids with different carbon chain length. Toxicology 184, 135-
688 140. http://dx.doi.org/10.1016/S0300-483X(02)00573-5.
689 Pan, C.G., Ying, G.G., Liu, Y.S., Zhang, Q.Q., Chen, Z.F., Peng, F.J., Huang, G.Y., 2014.
690 Contamination profiles of perfluoroalkyl substances in five typical rivers of the Pearl River
691 Delta region, South China. Chemosphere 114, 16-25. https://doi.org/10.1016/j.chemosphere.
692 2014.04.005.
693 Pan, G., You, C., 2010. Sediment-water distribution of perfluorooctane sulfonate (PFOS) in Yangtze
694 River Estuary. Env. Pollut. 158, 1363-1367. https://doi.org/10.1016/j.envpol.2010.01.011.
695 Panin, N., 2003. The Danube Delta. Geomorphology and Holocene Evolution: a synthesis/Le delta
696 du Danube. Géomorphologie et évolution holocène: une synthèse. Géomorphologie Reli.
697 Process. Environ. 9, 247-262. https://doi.org/10.3406/morfo.2003.1188.
698 Pasanisi, E., Cortés-Gómez, A.A., Pérez-López, M., Soler, F., Hernández-Moreno, D., Guerranti, C.,

699 Martellini, T., Fuentes-Mascorro, G., Romero, D., Cincinelli, A., 2016. Levels of
700 perfluorinated acids (PFCAs) in different tissues of Lepidochelys olivacea sea turtles from the
701 Escobilla beach (Oaxaca, Mexico). Sci. Total Environ. 572, 1059-1065.
702 https://doi.org/10.1016/j.scitotenv.2016.08.013.
703 Prevedouros. K., Cousins. T., 2006. Sources, fate and transport of perfluorocarboxylates. Environ.
704 Sci. Technol. 1, 32-44. https://doi.org/10.1002/chin.200611255.
705 Schwarzenbach, R.P., Escher, B.I., Fenner, K., Hofstetter, T.B., Johnson, C.A., Von Gunten, U.,
706 Wehrli, B., 2006. The challenge of micropollutants in aquatic systems. Science 313 (5790),
707 1072-1077. https://doi.org/10.1126/science.1127291.
708 Sedlak, M.D., Benskin, J.P., Wong, A., Grace, R., Greig, D.J., 2017. Per- and polyfluoroalkyl
709 substances (PFASs) in San Francisco Bay wildlife: Temporal trends, exposure pathways, and
710 notable presence of precursor compounds. Chemosphere 185, 1217-1226.
711 https://doi.org/10.1016/j.chemosphere.2017.04.096.
712 Sepulvado, J.G., Blaine, A.C., Hundal, L.S., Higgins, C.P., 2011. Occurrence and fate of
713 perfluorochemicals in soil following the land application of mu nicipal biosolids. Environ. Sci.
714 Technol. 45, 8106-8112. https://doi.org/10.1021/es103903d.
715 Sharma, B.M., Bharat, G.K., Tayal, S., Larssen, T., Bečanová, J., Karásková, P., Whitehead, P.G.,
716 Futter, M.N., Butterfield, D., Nizzetto, L., 2016. Perfluoroalkyl substances (PFAS) in river and
717 ground/drinking water of the Ganges River basin: emissions and implications for human
718 exposure. Environ. Pollut. 208, 704-713. https://doi.org/10.1016/j.envpol.2015.10.050.
719 Shi, Z., Ding, L., Zhang, H., Feng, Y., Xu, M., Dai, J., 2009. Chronic exposure to
720 perfluorododecanoic acid disrupts testicular steroidogenesis and the expression of related
721 genes in male rats. Toxicol. Lett. 188, 192-200. https://doi.org/10.1016/j.toxlet.2009.04.014.
722 Simcik, M.F., Dorweiler, K.J., 2005. Ratio of perfluorochemical concentrations as a tracer of
723 atmospheric deposition to surface waters. Environ. Sci. Technol. 39, 8678-8683.
724 https://doi.org/10.1021/es0511218.
725 So, M.K., Miyake, Y., Yeung, W.Y., Ho, Y.M., Taniyasu, S., Rostkowski, P., Yamashita, N., Zhou,
726 B.S., Shi, X.J., Wang, J.X., 2007. Perfluorinated compounds in the Pearl river and Yangtze
727 river of China. Chemosphere 68, 2085-2095. https://doi.org/10.1016/j.chemosphere.
728 2007.02.008.

729 So, M.K., Taniyasu, S., Yamashita, N., Giesy, J.P., Zheng, J., Fang, Z., 2004. Perfluorinated
730 compounds in coastal waters of Hong Kong, south China, and Korea. Environ. Sci. Technol.
731 38, 4056-4063. https://10.1021/es049441z.
732 Squadrone, S., Ciccotelli, V., Favaro, L., Scanzio, T., Prearo, M., Abete, M.C., 2014. Fish
733 consumption as a source of human exposure to perfluorinated alkyl substances in Italy:
734 analysis of two edible fish from Lake Maggiore. Chemosphere 114, 181-186.
735 https://10.1016/j.chemosphere.2014.04.085
736 Stockholm Convention on persistent organic pollutions (POPs), 2019.
737 http://chm.pops.int/TheConvention/Overview/TextoftheConvention/tabid/2232/Default.aspx.
738 (accessed 11 February 2020)
739 Stroski, K.M., Luong, K.H., Challis, J.K., Chaves-Barquero, L.G., Hanson, M.L., Wong, C.S., 2020.
740 Wastewater sources of per- and polyfluorinated alkyl substances (PFAS) and pharmaceuticals
741 in four Canadian Arctic communities. Sci. Total Environ. 708, 134494.
742 https://doi.org/10.1016/j.scitotenv.2019.134494.
743 Su, H.Q., Shi, Y.J., Lu, Y.L., Wang, P., Zhang, M., Andrew, S., Jones, K., Johnson, A., 2017. Home
744 produced eggs: An important pathway of human exposure to perfluorobutanoic acid (PFBA)
745 and perfluorooctanoic acid (PFOA) around a fluorochemical industrial park in China. Environ.
746 Int. 101, 1-6. https://10.1016/j.envint.2017.01.016.
747 Sun, H., Li, F., Zhang, T., Zhang, X., He, N., Song, Q., Zhao, L., Sun, L., Sun, T., 2011.
748 Perfluorinated compounds in surface waters and WWTPs in Shenyang, China: mass flows and
749 source analysis. Water Res. 45, 4483-4490. https://doi.org/10.1016/j.watres.2011.05.036.
750 Thompson, J., Roach, A., Eaglesham, G., Bartkow, M.E., Edge, K., Mueller, J.F., 2011.
751 Perfluorinated alkyl acids in water, sediment and wildlife from Sydney Harbour and
752 surroundings. Mar. Pollut. Bull. 62, 2869-2875.
753 https://doi.org/10.1016/j.marpolbul.2011.09.002.
754 United Nations Environment Programme (UNEP), 2009. Report of the conference of the parties of
755 the Stockholm Convention on persistent organic pollutants on the work of its fourth meeting.
756 http://chm.pops.int/Implementation/IndustrialPOPs/PFOS/Overview/tabid/5221/Default.aspx.
757 (accessed 11 February 2020)
758 USEPA, 2006. PFOA Stewardship Program. https://www.epa.gov/assessing-and-managing-

759 chemicals-under-tsca/risk-management-and-polyfluoroalkyl-substances-pfass#tab-3. (accessed
760 11 February 2020)
761 Wang, B., Cao, M., Zhu, H., Chen, J., Wang, L., Liu, G., Gu, X., Lu, X., 2013. Distribution of
762 perfluorinated compounds in surface water from Hanjiang River in Wuhan, China.
763 Chemosphere 93, 468-473. https://doi.org/10.1016/j.chemosphere.2013.06.014.
764 Wang, F., Shih, K., Ma, R., Li, X., 2015. Influence of cations on the partition behavior of
765 perfluoroheptanoate (PFHpA) and perfluorohexanesulfonate (PFHxS) on wastewater sludge.
766 Chemosphere 131, 178-183. https://doi.org/10.1016/j.chemosphere.2015.03.024.
767 Wang, Y., Fu, J., Wang, T., Liang, Y., Pan, Y., Cai, Y., Jiang, G., 2010. Distribution of
768 perfluorooctane sulfonate and other perfluorochemicals in the ambient environment around a
769 manufacturing facility in China. Environ. Sci. Technol. 44, 8062-8067.
770 https://doi.org/10.1021/es101810h.
771 Wilhelm, M., Bergmann, S., Dieter, H.H., 2010. Occurrence of perfluorinated compounds (PFCs) in
772 drinking water of North Rhine-Westphalia, Germany and new approach to assess drinking
773 water contamination by shorter-chained C4-C7 PFCs. Int. J. Hyg. Environ. Health 213, 224-
774 232. https://doi.org/10.1016/j.ijheh.2010.05.004.
775 Xie, S., Wang, T., Liu, S., Jones, K.C., Sweetman, A.J., Lu, Y., 2013. Industrial source identification
776 and emission estimation of perfluorooctane sulfonate in China. Environ. Int. 52, 1-8.
777 https://doi.org/10.1016/j.envint.2012.11.004.
778 Xu, K., Milliman, J.D., 2009. Seasonal variations of sediment discharge from the Yangtze River
779 before and after impoundment of the Three Gorges Dam. Geomorphology 104, 276-283.
780 https://doi.org/10.1016/j.geomorph.2008.09.004.
781 Xu, X.J., Yang, S.L., Zhang, Z., 2010. Variation in grain size of sediment in middle and lower
782 Changjiang River since impoundment of Three Gorges Reservoir. Sci. Geogr. Sin. 30, 103-
783 107. (in Chinese)
784 Yang, S.L., Milliman, J.D., Xu, K.H., Deng, B., Zhang, X.Y., Luo, X.X., 2014. Downstream
785 sedimentary and geomorphic impacts of the Three Gorges Dam on the Yangtze River. Earth-
786 Science Rev. 138, 469-486. https://doi.org/10.1016/j.earscirev.2014.07.006.
787 Yang, S.L., Zhang, J., Xu, X.J., 2007. Influence of the Three Gorges Dam on downstream delivery
788 of sediment and its environmental implications, Yangtze River. Geophys. Res. Lett. 34 (10),

789 L10401. https://doi.org/10.1029/2007GL029472.
790 Yang, Z.S., Wang, H.J., Saito, Y., Milliman, J.D., Xu, K., Qiao, S., Shi, G., 2006. Dam impacts on
791 the Changjiang (Yangtze) River sediment discharge to the sea: The past 55 years and after the
792 Three Gorges Dam. Water Resour. Res. 42, W04407. https://doi.org/10.1029/2005WR003970.
793 You, C., Jia, C., Pan, G., 2010. Effect of salinity and sediment characteristics on the sorption and
794 desorption of perfluorooctane sulfonate at sediment-water interface. Environ. Pollut. 158,
795 1343-1347. https://doi.org/10.1016/j.envpol.2010.01.009.
796 Zhang L., Liu J.G., Hu J.X., Liu C., Guo W.G., Wang Q., Wang H., 2012. The inventory of sources,
797 environmental releases and risk assessment for perfluorooctane sulfonate in China. Environ.
798 Pollut. 165, 193-198. https://doi.org/10.1016/j.envpol.2011.09.001.
799 Zhang, W., Zhang, Y., Taniyasu, S., Yeung, L. W.Y., Lam, P.K.S., Wang, J., 2013. Distribution and
800 fate of perfluoroalkyl substances in municipal wastewater treatment plants in economically
801 developed areas of china. Environ. Pollut. 176, 10-17.
802 https://doi.org/10.1016/j.envpol.2012.12.019.
803 Zhao, L., Zhu, L., Yang, L., Liu, Z., Zhang, Y., 2012. Distribution and desorption of perfluorinated
804 compounds in fractionated sediments. Chemosphere 88, 1390-1397. https://doi.org/10.1016/j.
805 chemosphere.2012.05.062.
806 Zheng, G.M., Miller, P., von Hippel, F.A., Buck, C.L., Carpenter, D.O., Salamova, A., 2020. Legacy
807 and emerging semi-volatile organic compounds in sentinel fish from an arctic formerly used
808 defense site in Alaska. Environ. Pollut. 259, 113872.
809 https://doi.org/10.1016/j.envpol.2019.113872.
810 Zhou, Z., Liang, Y., Shi, Y., Xu, L., Cai, Y., 2013. Occurrence and transport of perfluoroalkyl acids
811 (PFAAs), including short-chain PFAAs in Tangxun Lake, China. Environ. Sci. Technol. 47,
812 9249-9257. https://pubs.acs.org/doi/10.1021/es402120y.
813

814 Table 1 Contents and detection frequencies of PFASs in water (ng/L) and sediment (μg/kg) of the

815 Yangtze River in spring and autumn

816

817

Matrix	Season		PFOA	PFHxA	PFBS	PFHpA	PFHxS	PFNA	PFDA	PFOS	PFUnDA	PFDoDA	PFTeDA	∑11 PFASs
Water	Spring	Range	ND-86.90	ND-14.92	ND-0.78	ND-3.47	ND-0.66	ND-1.34	ND-1.18	ND-2.93	ND-2.68	ND-1.00	ND-0.36	0.30-88.50
		Mean	33.30	ND	0.27	ND	ND	0.06	ND	0.13	ND	0.12	ND	16.17
		Median	4.38	ND	0.25	ND	ND	ND	ND	ND	ND	0.05	ND	7.74
		DF	95.3	20.9	97.7	7.0	51.2	32.6	27.9	20.9	2.3	55.8	39.5	100
	Autumn	Range	ND-62.85	ND-4.57	ND-4.61	ND-0.35	ND-3.27	ND-0.22	ND-0.06	ND-4.54	ND-0.71	ND-0.42	ND-0.92	ND-68.78
		Mean	9.38	ND	0.88	ND	0.24	ND	ND	0.95	0.028	0.08	0.20	11.89
		Median	2.08	ND	0.26	ND	ND	ND	ND	0.39	ND	ND	ND	8.69
		DF	93.0	4.7	100	2.3	67.4	25.6	16.3	62.8	9.3	53.5	62.8	100
Sediment	Spring	Range	ND-0.94	2.43-89.68	ND-4.92	ND-50.80	ND-0.74	ND-0.92	ND-1.76	ND-4.60	ND-0.64	ND-0.47	ND-1.74	ND-151.65
		Mean	0.16	14.58	0.53	11.56	0.23	0.20	0.43	1.26	0.23	0.14	0.52	31.53
		Median	0.15	6.62	0.31	6.82	0.20	0.34	0.31	0.87	0.20	0.12	0.43	19.52
		DF	94.5	100	94.5	100	89.1	98.2	98.2	100	100	100	100	100
	Autumn	Range	ND	0.31-65.22	ND-1.36	ND-35.51	ND-0.41	ND-0.11	ND-0.58	ND-0.51	ND-0.01	ND-0.06	ND-0.30	ND-96.90
		Mean	ND	11.09	0.16	5.95	ND	ND	ND	0.13	ND	ND	0.17	20.15
		Median	ND	1.52	ND	1.38	ND	ND	ND	0.13	ND	ND	0.17	3.08
		DF	0	100	27.3	100	21.8	25.5	54.5	74.5	3.6	3.6	100	100

818 2 ND: not detected; DF: detection frequency (%).

819

820

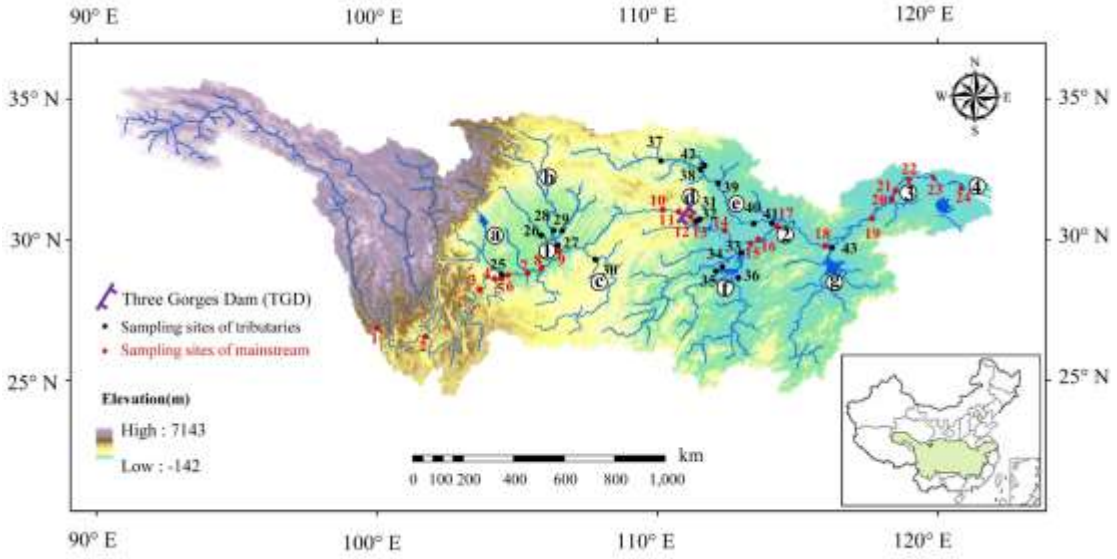

Fig. 1 Map of water and sediment sampling sites along the Yangtze River (43 monitoring stations cover a stream-wise length of 4300 km. Table S1 lists detailed information on the (numbered) sampling sites). Red dots represent sampling sites in the mainstream, black dots indicate sampling sites in tributaries. Letters with circles refer to the following main tributaries and lakes: ⓐ Minjiang, ⓑ Jialingjiang, ⓒ Wujiang, ⓓ Huangbaihe, ⓔ Hanjiang, ⓕ Dongting Lake, and ⓖ Poyang Lake. Numbers with circles refer to the following large cities: ① Chongqing, ② Wuhan, ③ Nanjing, and ④ Shanghai.

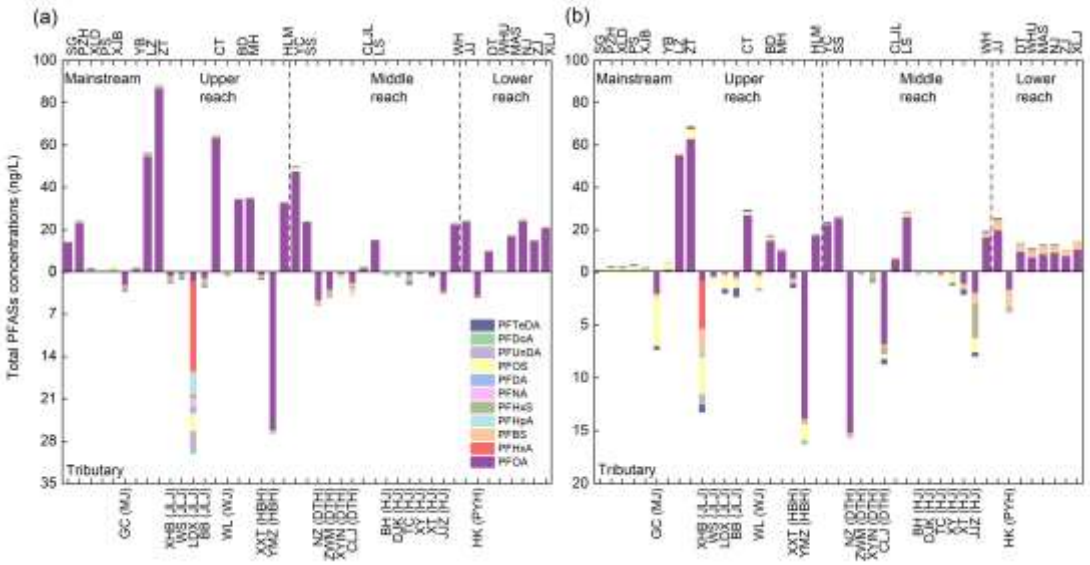

Fig. 2 Total PFASs concentrations (ng/L) in surface water samples taken from the Yangtze River in (a) spring and (b) autumn. Upright bars refer to the mainstream, and inverted bars refer to individual tributaries)

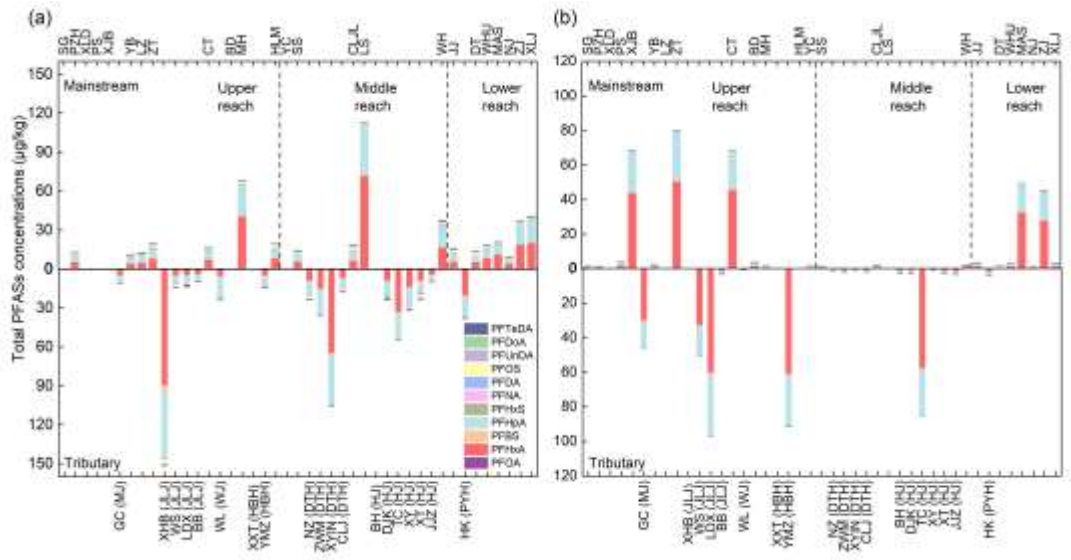

Fig. 3 Total PFASs concentrations (μg/kg) in sediment samples taken from the Yangtze River in (a) spring and (b) autumn. Upright bars refer to the mainstream, and inverted bars refer to individual tributaries)

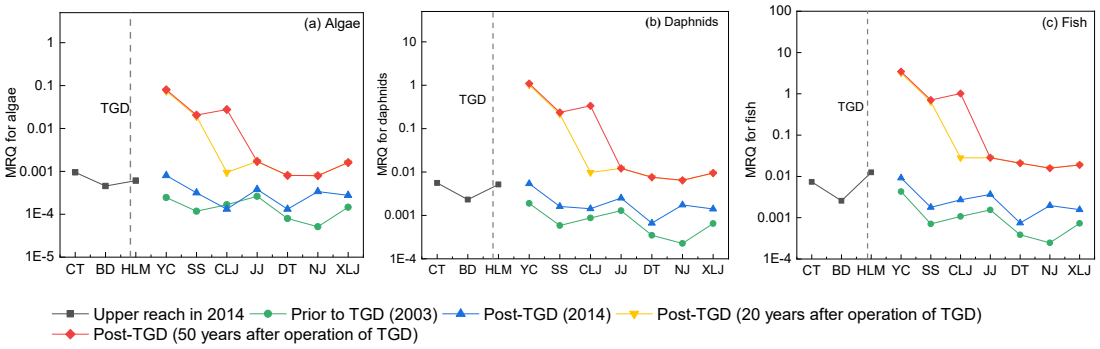

Fig. 4 Mixture risk quotients (MRQs) for (a) algae, (b) daphnids, and (c) fish in water samples taken in spring for three scenarios assuming constant input of PFASs into the river over the period of interest (50 years after initial operation of TGD).

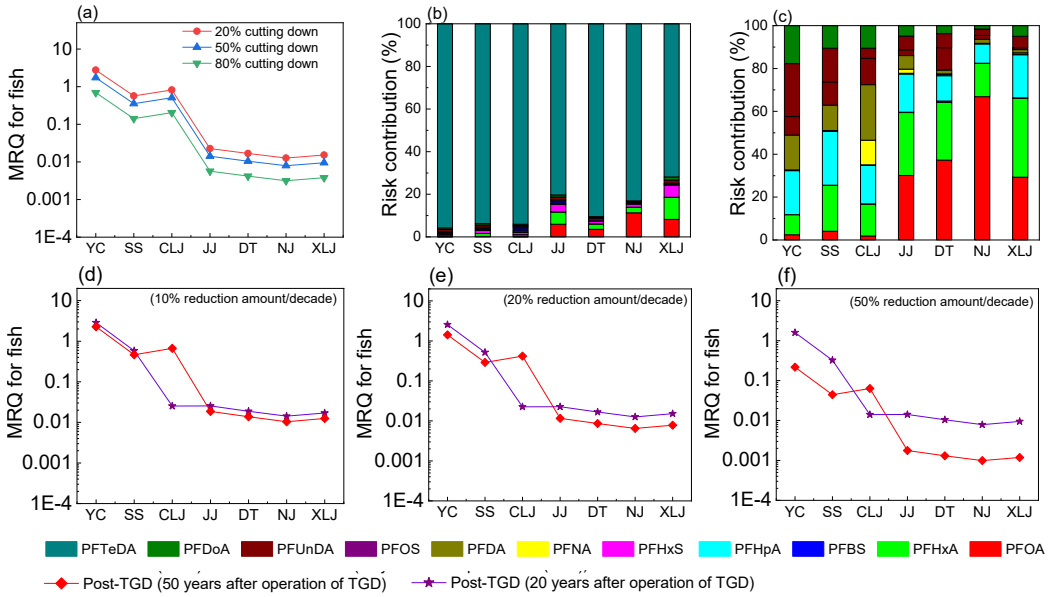

Fig. 5 Risk assessment for fish in the Yangtze river experiencing future scenarios related to different control strategies for PFASs. Panels a, b and c refer to a future scenario, 50 years after operation of TGD, with reduced total PFASs input into the Yangtze River: (a) MRQs with 20%, 50% and 80% abrupt decadal reductions in PFASs; (b) Risk contribution (%) of individual PFAS for 80% reduction in overall PFASs; (c) Risk contribution (%) of individual PFAS (excluding PFTeDA) with 80% reduction in overall PFASs. Panels d, e and f refer to future scenarios, 20 and 50 years after operation of TGD, for the following reduction rates in PFASs: (a) 10%, (b) 20%, and (c) 50% reduction per decade from 2015.

866

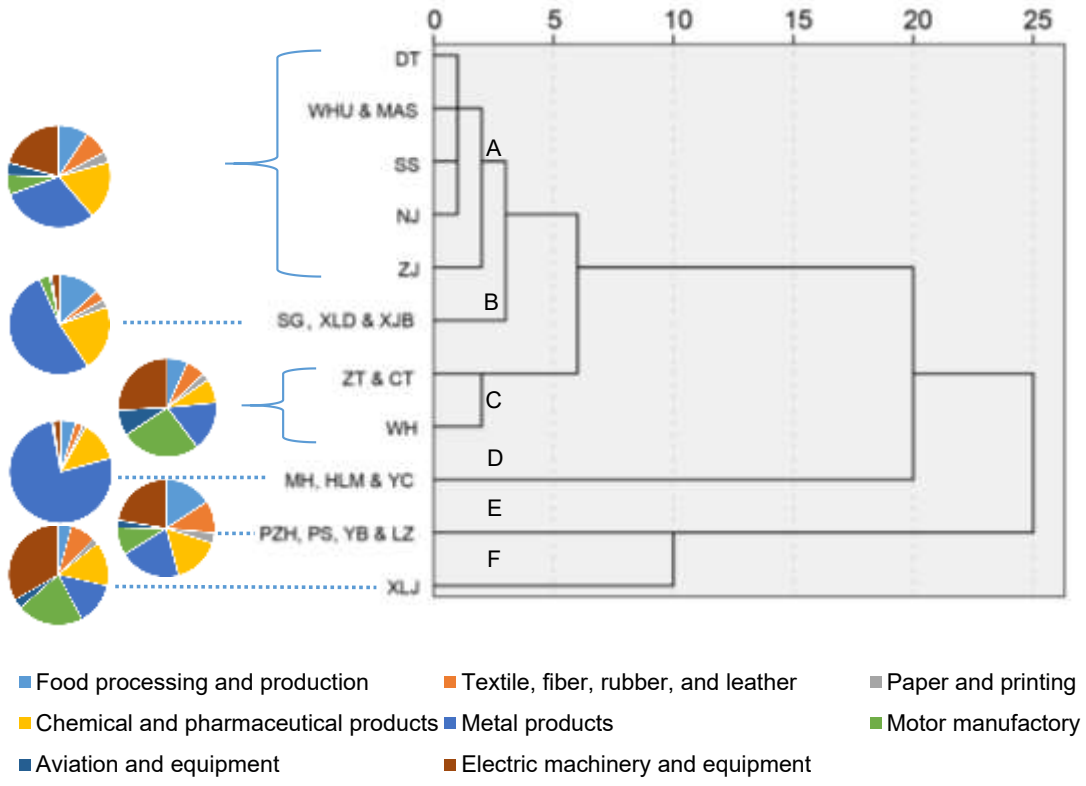

867

868

869 Fig. 6 Cluster analysis of PFASs-related industries along the mainstream of the Yangtze River

870